ECG-based Assessment and Therapeutic Implications of AV Nodal Conduction Dynamics During Atrial Fibrillation

Mattias Karlsson[1,2], Mikael Wallman[1], Pyotr G Platonov[3], Sara R. Ulimoen[4], Frida Sandberg[2]

[1] Dept. of Systems and Data Analysis, Fraunhofer-Chalmers Centre, Gothenburg, Sweden
[2] Dept. of Biomedical Engineering, Lund University, Lund, Sweden
[3] Dept. of Cardiology, Clinical Sciences, Lund University, Lund, Sweden
[4] Vestre Viken Hospital Trust, Bærum Hospital, Rud, Norway

Abstract

The conduction properties of the atrioventricular (AV) node have a significant impact on heart rate during permanent atrial fibrillation (AF), and can be modulated through the use of β-blockers or calcium channel blockers. These drugs have different physiological effects and are often selected empirically. Hence, an improved understanding of how these drugs affect the AV node conduction properties may contribute to personalized treatment of AF.

We propose a novel methodology for estimating the refractory period and conduction delay dynamics of the fast and slow pathways of the AV node from 24-hour ambulatory ECG recordings. Our approach comprises a network model of the AV node, a problem-specific genetic algorithm, and an approximate Bayesian computation algorithm for estimating the posterior distribution of the AV node properties.

We analyzed 24-hour ambulatory ECG recordings at baseline from 51 patients with permanent AF. Interestingly, a moderate correlation between the short-term variability in the refractory period for the fast pathway and reduction in heart rate during treatment with metoprolol ($\rho = 0.48, p < 0.005$) was found. Thus, the proposed methodology enables individualized characterization of the AV node and can potentially assist in treatment selection.

1. Introduction

Atrial fibrillation is the most common sustained cardiac arrhythmia and significantly burdens patients and the healthcare system at large [1]. During AF, the electrical activity in the atria is highly disorganized, leading to rapid and irregular contraction of the atria. The ventricles are partly protected from rapid atrial impulses by the atrioventricular node due to its ability to block and delay incoming impulses.

Nevertheless, the blocking and delay in the AV node are often insufficient to maintain a healthy heart rate. Hence, treatment with rate control drugs modifying the AV node conduction in order to lower the pulse is common for patients suffering from permanent AF. However, the treatment choice between the two recommended drug types – β-blockers and calcium channel blockers – is made empirically [1]. The two drug types have different physiological effects, hence treatment with different drug types can have different outcomes on an individual level. Thus, individual characterization of the AV node can potentially assist in treatment selection.

We have previously proposed a network model of the AV node including the refractory period and conduction delay in the fast pathway (FP) and the slow pathway (SP) [2], as well as a framework for estimating the model parameters during 24 hours using non-invasive data [3]. However, the interpretation of the AV node assessment was limited by the number of model parameters and their intrinsic complex dependencies. For use in a clinical context, the outcome needs to be readily interpretable by medical professionals. In addition, only one estimated value was produced, limiting the understanding of the estimates.

In this study, we propose a novel methodology for estimating the refractory period and conduction delay of the fast and slow pathway of the AV node continuously over 24 hours for 51 patients during baseline using the network model. The estimates comprise samples from the Bayesian posterior distribution of the AV node properties, hereafter denoted the posterior. This analysis enables the identification of correlations between the estimated AV node properties for a patient and their response to pharmacological interventions with four different rate control drugs.

2. Method

The method for assessing the refractory period and conduction delay in both pathways of the AV node can be divided into four stages: (1) ECG processing to derive RR interval series and an atrial fibrillatory rate (AFR) (Sec. 2.1); (2) Rough model parameter estimation using a problem-specific genetic algorithm (GA) (Sec. 2.3.1); (3) Computa-

tion of the posterior using approximate Bayesian computation (ABC) (Sec. 2.3.2); (4) Translation from the original model parameters ($\boldsymbol{\theta}$) to estimates of the refractory period and conduction delay ($\boldsymbol{\Phi}$) (Sec. 2.3.3).

2.1. ECG processing

We analyzed 24-hour ambulatory ECGs from 60 patients with permanent AF from the RATAF study [4]. Data were obtained during baseline and treatment with verapamil and diltiazem (calcium channel blockers) and metoprolol and carvedilol (β-blockers).

The RR interval series is extracted from the ECG for each patient and segmented into ten-minute intervals with a five-minute overlap. The f-waves are extracted from the ECGs using spatiotemporal QRST cancellation and used to estimate the AFR trends by a hidden Markov model-based approach [5]. The AFR trends are divided into segments corresponding to those of the RR interval series. Segments with excessive noise, preventing beat detection and AFR trend estimation, are excluded from further analysis; resulting in 51 patients with RR interval series and AFR trends with a duration of over 20 hours. In addition, the change in the 24-hour average heart rate (ΔHR) in response to treatment with all four treatments is calculated.

2.2. Network Model of the AV Node

The model of the AV node is divided into the FP and the SP, where each pathway comprises 10 nodes corresponding to a localized section of the AV node [2]. The pathways are connected by a coupling node, representing the Bundle of His and the Purkinje fibers, as illustrated in Figure 1. The input to the model, representing the atrial impulse arrival time, is created by a Poisson process with mean arrival rate λ. Each node will either block an incoming impulse – if the node is in its refractory state – or transmit it to all adjacent nodes with an added conduction delay. The refractory period ($R_i(n)$) and conduction delay ($D_i(n)$) for node i are updated for each incoming impulse n according to Equation 1, 2, and 3.

$$R_i(n) = R_{min} + \Delta R(1 - e^{-\tilde{t}_i(n)/\tau_R}) \quad (1)$$

$$D_i(n) = D_{min} + \Delta D e^{-\tilde{t}_i(n)/\tau_D}, \quad (2)$$

$$\tilde{t}_i(n) = t_i(n) - t_i(n-1) - R_i(n-1), \quad (3)$$

Here, $\tilde{t}_i(n)$ is the diastolic interval preceding impulse n and $t_i(n)$ is the arrival time of impulse n at node i. Additionally, when $\tilde{t}_i(n)$ is negative, the node is refractory and will block incoming impulses. The refractory period and conduction delay are thus defined by R_{min}, ΔR, τ_R, D_{min}, ΔD, and τ_D; which are assumed to be identical for the nodes in the respective pathway. This results in the 12 model parameters $\boldsymbol{\theta} = [R^{FP}_{min}, \Delta R^{FP}, \tau^{FP}_R, R^{SP}_{min}, \Delta R^{SP}, \tau^{SP}_R, D^{FP}_{min}, \Delta D^{FP}, \tau^{FP}_D, D^{SP}_{min}, \Delta D^{SP}, \tau^{SP}_D]$. The refractory period in the coupling node is fixed to the mean of the ten shortest RR intervals in the current data, and its conduction delay is fixed at 60 ms.

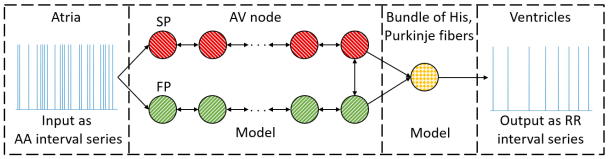

Figure 1: A schematic representation of the network model with arrows indicating impulse conduction direction, divided into the SP nodes (red), FP nodes (green), and the coupling node (yellow).

2.3. Parameter estimation

The mean arrival rate for the Poisson process λ and the model parameters $\boldsymbol{\theta}$ are estimated for each ten-minute segment. The mean arrival rate λ is estimated as the mean of the AFR trend in each segment, and $\boldsymbol{\theta}$ is estimated using a problem-specific GA together with an ABC algorithm.

An error function (ϵ) based on the Poincaré plot, i.e., the scatter plot of successive pairs of RR intervals, is used to quantify the difference between the extracted RR interval series in each segment and the model output. The extracted and simulated RR intervals are placed in two-dimensional bins centered between 250 and 1800 ms with a width of 50 ms, resulting in K = 961 bins. The error function is computed according to Equation 4,

$$\epsilon = \frac{1}{K} \sum_{k=1}^{K} \frac{\left(x_k - \frac{1}{t_{norm}} \tilde{x}_k\right)^2}{\sqrt{x_k}}, \quad (4)$$

where $\tilde{x}_k$ and x_k are the numbers of RR intervals in the k-th bin of the simulated and observed data, respectively. Further, t_{norm} is used to normalize the simulated data to match the length of the ten-minute-long observed data.

2.3.1. Genetic algorithm

A problem-specific dynamic GA based on the work in [3] is used to get the rough estimate of $\boldsymbol{\theta}$ for initialization in the ABC algorithm. The GA uses a population of 300 individuals, where each individual is a vector of values for $\boldsymbol{\theta}$. The algorithm uses tournament selection, a two-point crossover, and creep mutation. To increase performance, immigration through replacement of the least-fit individuals in the population, as well as tuning the hyper-parameters during the optimization, is performed. In addition, the number of generations the GA runs before moving to the next data segment also varies during the optimization, ranging from two to seven. For further details about the algorithm, see [3].

2.3.2. Approximate Bayesian computation

To estimate the posterior ($p(\boldsymbol{\theta}|RR(s), \lambda(s))$) of $\boldsymbol{\theta}$ knowing the RR interval series ($RR(s)$) and $\lambda(s)$ in a segment s, an

approximate Bayesian computation population Monte Carlo sampling (ABC PMC) algorithm is used [6]. The posterior for each segment is estimated individually by running the ABC PMC using $N_p = 100$ particles for eight iterations (j), where each particle is a vector of values for $\boldsymbol{\theta}$. During each iteration, each particle has a probability of being chosen based on the covariance of the particles, and the chosen particle is perturbed using a normal distribution to create a proposal. If the proposal error ϵ is lower than a threshold T_j, the proposal is accepted. The next iteration starts when N_p particles are accepted. The threshold is updated for each new iteration based on the results from the GA, where T_1 is set to ϵ of the tenth fittest individual in the GA, T_2 to the eighth, T_3 to the fifth, T_4 to the third, and T_{5-8} to ϵ of the fittest individual. The algorithm is sped up by utilizing the GA results to create the initial population by sampling twenty particles from five different normal distributions in order to construct the initial population. The mean of these distributions ranges from the first to the fifth fittest individual in the GA, and the standard deviation for all five distributions is set to the standard deviation of the 25 fittest individuals in the GA. For further details about the algorithm, see [7].

2.3.3. Parameter reduction

The resulting 100 particles from the ABC PMC algorithm are used as an estimate of the posterior of $\boldsymbol{\theta}$ in each data segment. The particles are used in the model to simulate ten-minute-long segments of data, where all $R_i(n)$ and $D_i(n)$ for each pathway are stored. This thus creates samples from a distribution of the refractory period and conduction delay for each pathway and segment, which we denote $\hat{\boldsymbol{\Phi}}(pat, s) = [\boldsymbol{R}^{FP}, \boldsymbol{R}^{SP}, \boldsymbol{D}^{FP}, \boldsymbol{D}^{SP}]$. These correspond to a translation from the twelve model parameters $\boldsymbol{\theta}$ to the more interpretable AV node properties $\hat{\boldsymbol{\Phi}}$. The distributions are quantified using the maximum of the empirical probability density function, as well as the 5% and 95% credibility region limits; denoted as $\hat{\boldsymbol{\phi}}_{max}(pat, s) = [R^{FP}_{max}, R^{SP}_{max}, D^{FP}_{max}, D^{SP}_{max}]$ and $\hat{\boldsymbol{\phi}}_{95,5}(pat, s) = [R^{FP}_{95,5}, R^{SP}_{95,5}, D^{FP}_{95,5}, D^{SP}_{95,5}]$ for each segment s and patient pat, where 95 or 5 indicates the credibility region limit. In addition, the number of impulses traveling through the two pathways (N_{FP}, N_{SP}) is stored and their ratio is denoted $SP_{ratio} = \frac{N_{SP}}{N_{FP}+N_{SP}}$.

3. Results

The resulting 24-hour trends of $\hat{\boldsymbol{\phi}}_{max}(pat, s)$ and $\hat{\boldsymbol{\phi}}_{95,5}(pat, s)$ for one patient are shown in Figure 3. Interestingly, R_{FP} is very uncertain during nighttime, whereas R_{SP} is increased and its short-term variation is lowered compared to daytime. In fact, the credibility region in R_{FP} and D_{FP} is larger compared to R_{SP} and D_{SP} for this patient, probably due to the smaller number of impulses conducted through the FP, as seen in the SP_{ratio}.

The average values for $\hat{\boldsymbol{\phi}}_{max}(pat, s)$ and the 90% credibility region for all patients are shown in Table 1. It is evident that the credibility region for R_{FP} is larger compared to R_{SP}, reflecting the results in Figure 3. In addition, the credibility region for D_{FP} in proportion to its mean value is larger than that of D_{SP}. Moreover, the mean $\pm$ std for the SP_{ratio} is 0.78 ± 0.10. Hence, the SP is on average the dominant pathway, which is also reflected in the larger credibility regions for the FP.

Table 1: The mean $\pm$ std of the average $\hat{\boldsymbol{\phi}}_{max}(pat, s)$ and the 95% credibility region for all patients, where the total delay for all ten nodes in each pathway is presented

	R^{FP} (ms)	R^{SP} (ms)	$10D^{FP}$ (ms)	$10D^{SP}$ (ms)
$\overline{\hat{\boldsymbol{\phi}}}_{max}(pat, s)$	934 ± 203	399 ± 95	76.9 ± 47.6	546 ± 126
$\overline{\hat{\boldsymbol{\phi}}}_{95}(pat, s) - \overline{\hat{\boldsymbol{\phi}}}_{5}(pat, s)$	687 ± 232	217 ± 114	304 ± 111	447 ± 103

The maximal distance between the cumulative distribution functions of the AV node properties for consecutive segments, i.e. the Kolmogorov-Smirnov (KS) distance, is used to quantify the variation in $\hat{\boldsymbol{\phi}}_{max}(pat, s)$. The average KS distance ($\overline{\Delta KS}$) for each patient thus captures short-time variability in the trends. Figure 2 shows the resulting $\overline{\Delta KS}$ in R_{FP} for all patients plotted against the treatment effect ΔHR in response to the four rate control drugs.

According to the Henze-Zirkler test ($p < 0.05$), the data in Figure 2 do not follow a normal distribution. Hence, the Spearman's rank correlation is used to study the relationship, showing that $\overline{\Delta KS}$ at baseline has a moderate correlation with ΔHR during treatment with metoprolol ($\rho = 0.47, p < 0.005$), and no correlation during treatment with verapamil, diltiazem, or carvedilol. This relation also holds true for D_{FP}, where a weak correlation could be seen for metoprolol ($\rho = 0.35, p < 0.05$). More detailed results are found in [7].

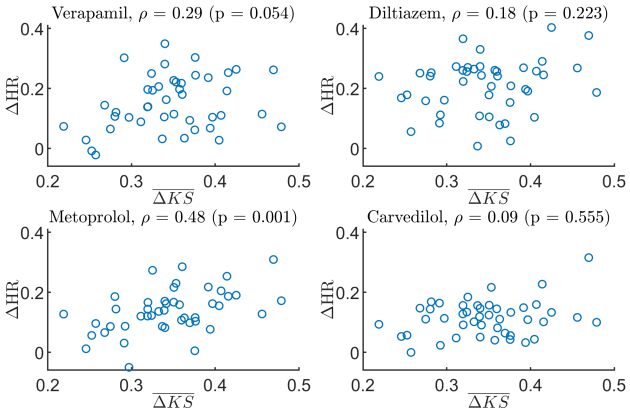

Figure 2: The relation between ΔHR and $\overline{\Delta KS}$ for R^{FP}.

4. Discussion

The results in Figure 2 show a significant correlation between the short-term variations in R^{FP} and ΔHR for metoprolol, but not for verapamil, diltiazem, or carvedilol. From a physiological viewpoint, β-blockers could be expected to have a stronger effect on patients with large variations in the AV node properties, indicating a strong influence of the autonomic nervous system. This would explain the high correlation between short-time variation and treatment effect during treatment with metoprolol, as seen in Figure 2. The absence of a strong correlation for carvedilol might be due to the low overall effect carvedilol showed in the RATAF study, possibly due to its rapid elimination, which has previously been pointed out as a limitation in the RATAF study [8].

The advantage of estimating the posterior compared to a single optimal value of the AV node properties can be understood by studying Figure 3, where R^{FP} during the night is very uncertain. Thus, the information in R^{FP} during the night is very limited. If the uncertainty was unknown, these uncertain estimates could influence decision-making or further analysis of the trends, hindering the usefulness of the estimates.

Previous versions of the model and framework [3] estimated the model parameters as opposed to the AV node properties, limiting the interpretability. In contrast, this work allows for a single estimate of the refractory period and conduction delay for each time instance. Deriving interpretable estimates is important for communicating analysis results and opens up the possibility for a deeper understanding of the AV node and its long and short-term variations.

The limited number of patients combined with the large inter-individual variability restricts the generality of the findings, thus more data are necessary to verify the results. Additionally, it should be noted that the estimated conduction properties have not been validated against intracardiac measurements, since no clinical standard exists to obtain this information during AF.

5. Conclusion

A method for estimating 24-hour trends of the refractory period and conduction delay in both pathways of the AV node together with an estimate of the associated uncertainty has been developed for patients with permanent AF.

Preliminary results suggest that short-term variation in the fast pathway refractoriness and conduction delay may be predictive of treatment outcome, indicating a possibility for personalized assistance in treatment selection.

References

[1] Hindricks G, et al. 2020 ESC guidelines for the diagnosis and management of atrial fibrillation developed in collaboration with the european association of cardio-thoracic surgery (EACTS). Am J Physiol Heart Circ Physiol 2020;.

[2] Karlsson M, et al. Non-invasive characterization of human AV-nodal conduction delay and refractory period during atrial fibrillation. Front Physiol 2021;1849.

[3] Karlsson M, et al. ECG based assessment of circadian variation in AV-nodal conduction during AF – influence of rate control drugs. Frontiers in Physiology 2022;2015.

[4] Ulimoen SR, et al. Comparison of four single-drug regimens on ventricular rate and arrhythmia-related symptoms in patients with permanent atrial fibrillation. Am J Cardiol 2013; 111(2):225–230.

[5] Sandberg F, et al. Frequency tracking of atrial fibrillation using hidden markov models. IEEE Trans Biomed Eng 2008; 55(2):502–511.

[6] Beaumont MA, et al. Adaptive approximate bayesian computation. Biometrika 2009;96(4):983–990.

[7] Karlsson M, et al. Model-based estimation of AV-nodal refractory period and conduction delay trends from ECG. arXiv preprint arXiv231011223 2023;.

[8] Shapiro MA. Using equivalent doses of medications to convert atrial fibrillation. American Journal of Cardiology 2013; 111(10):1539.

Address for correspondence:

Mattias Karlsson

Chalmers Science Park SE-412 88 Göteborg, Sweden

Mattias.Karlsson@fcc.chalmers.se

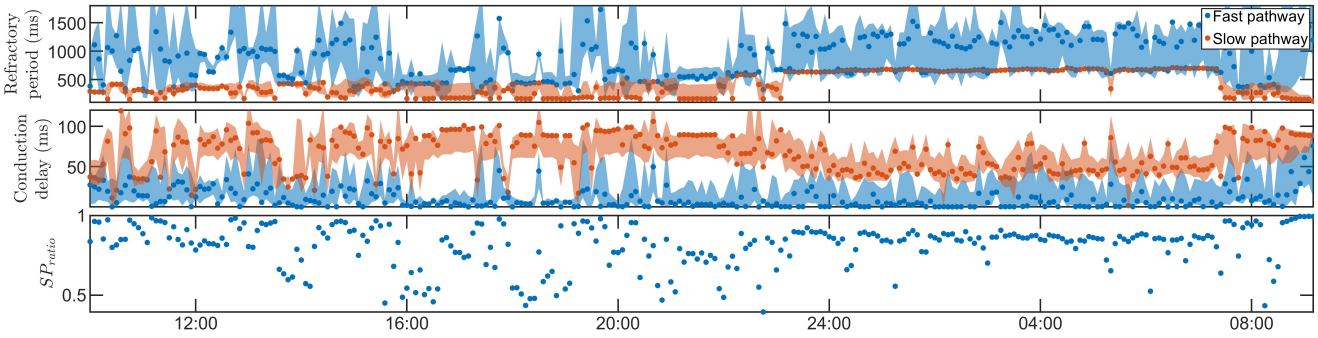

Figure 3: The estimated refractory period (top) and conduction delay (middle) for $\hat{\phi}_{max}(pat, s)$ (dotted) and $\hat{\phi}_{95,5}(pat, s)$ (filled) for the FP (blue) and SP (red), as well as the SP ratio (bottom) are shown for one example patient.